General Disclaimer

One or more of the Following Statements may affect this Document

- This document has been reproduced from the best copy furnished by the organizational source. It is being released in the interest of making available as much information as possible.

- This document may contain data, which exceeds the sheet parameters. It was furnished in this condition by the organizational source and is the best copy available.

- This document may contain tone-on-tone or color graphs, charts and/or pictures, which have been reproduced in black and white.

- This document is paginated as submitted by the original source.

- Portions of this document are not fully legible due to the historical nature of some of the material. However, it is the best reproduction available from the original submission.

Produced by the NASA Center for Aerospace Information (CASI)

DAA/Langley

VIRGINIA POLYTECHNIC INSTITUTE AND STATE UNIVERSITY

ENGINEERING SCIENCE AND MECHANICS DEPARTMENT

BLACKSBURG, VIRGINIA 24061 .

A Progress Report on

IDENTIFICATION AND CONTROL OF STRUCTURES IN SPACE

NASA Research Grant NAG-1-225

Covering the Period

January 1 - June 30, 1985

Principal Investigator: Leonard Meirovitch
                         University Distinguished Professor

Graduate Research Assistants: Roger D. Quinn
                               Mark A. Norris

Abstract

Work during the period January 1 - June 30, 1985, has concentrated on the completion of the derivation of the equations of motion for the Spacecraft Control Laboratory Experiment (SCOLE) as well on the development of a control scheme for the maneuvering of the spacecraft. The report consists of a paper presented at the Fifth VPI&SU/AIAA Symposium on Dynamics and Control of Large Structures, June 12-14, 1985, Blacksburg, VA.

MANEUVERING OF FLEXIBLE SPACECRAFT WITH APPLICATION[*]
TO SCOLE

by

L. Meirovitch, R. D. Quinn and M. A. Norris
Department of Engineering Science and Mechanics
Virginia Polytechnic Institute and State University
Blacksburg, Virginia 24061

Abstract

This paper is concerned with the derivation of the equations of motion for the Spacecraft Control Laboratory Experiment (SCOLE). For future reference, the equations of motion of a similar structure orbiting the earth are also derived. The structure is assumed to undergo large rigid-body maneuvers and small elastic deformations. A perturbation approach is presented where the quantities defining the rigid-body maneuver are assumed to be relatively large, with the elastic deformations and deviations from the rigid-body maneuver being relatively small. The perturbation equations have the form of linear, non-self-adjoint equations with time-dependent coefficients. An active control technique can then be formulated to permit maneuvering of the spacecraft and simultaneously suppressing the elastic vibration.

1. Introduction

⏤Some of the contemplated NASA missions involve experiments consisting of the control of flexible bodies carried by the shuttle in an earth orbit. Other missions involve laboratory simulations of similar experiments. Hence, a formulation capable of accommodating both types of experiments is desirable. To this end, we propose to derive Lagrange's equations of motion for the spacecraft of Fig. 1 regarding the structure as orbiting about the earth and then modify these equations so as to describe the laboratory experiment. In the derivation, the shuttle is treated as a rigid body and the beam and antenna as flexible, distributed-parameter members. The equations of motion can be further modified for the case of a rigid antenna.

The equations describing the maneuvering of a rigid space structure consist of nonlinear ordinary differential equations. On the other hand, the equations describing the small elastic displacements of a flexible structure relative to the rigid-body maneuver are linear

partial differential equations. Hence, the complete equations of motion describing a flexible body during a maneuver represent a set of nonlinear hybrid differential equations.

Hybrid systems possess an infinite number of degrees of freedom. In practice, however, it is necessary to reduce the number of degrees of freedom to a finite one, which implies spatial discretization and truncation. Substructure synthesis often proves useful as a method of discretization and truncation, particularly in the case of distributed substructures. Even in the case of discrete substructures, a set of linearly independent vectors can be used as admissible vectors to reduce the number of equations of motion.

In this paper, we propose a perturbation technique whereby the flexible spacecraft maneuver is assumed to consist of a combination of a rigid-body maneuver and small perturbations, including rigid-body deviations from the rigid-body maneuver and elastic vibrations. Regarding the rigid-body maneuver as known, the perturbation equations for the vibration control reduce to a set of linear ordinary differential equations with known time-varying coefficients.

2. Equations of Motion of the Spacecraft

It is convenient to refer the motion of the spacecraft to a given reference frame $x_0 y_0 z_0$, where the frame can be regarded as being embedded in the rigid shuttle. The reference frame has six degrees of freedom, three rigid-body translations and three rigid-body rotations.

We propose to derive the equations of motion by means of the Lagrangian approach. To this end, we must first obtain expressions for the kinetic energy, the potential energy and the virtual work. Considering Fig. 1 and denoting the position of the origin O of the frame $x_0 y_0 z_0$ by the vector $\underline{R}$ and the position of a point S in the shuttle relative to O by $\underline{r}$, the position of S relative to the inertial frame XYZ is $\underline{R}_S = \underline{R} + \underline{r}$. Moreover, denoting by $\underline{a}$ the vector from O to a nominal point A on the appendage and by $\underline{u}$ the elastic displacement vector of the point, the position of A in the displaced configuration is $\underline{R}_A = \underline{R} + \underline{a} + \underline{u}$. It must be noted that the vectors $\underline{r}$, $\underline{a}$ and $\underline{u}$ are likely to be measured relative to axes $x_0 y_0 z_0$. In view of the above, the velocity of a point S in the shuttle is

$$\dot{\underline{R}}_S = \dot{\underline{R}} + \underline{\omega} \times \underline{r} \tag{1}$$

where $\dot{\underline{R}}$ is the translational velocity and $\underline{\omega}$ is the angular velocity of the frame $x_0 y_0 z_0$ with respect to the inertial frame. Similarly, the

velocity of a point A in the appendage is

$$\dot{R}_A = \dot{R} + \omega \times (a + u) + \dot{u} \tag{2}$$

where $\dot{u}$ is the elastic velocity of the point relative to the $x_0 y_0 z_0$ frame. Hence, the kinetic energy of the spacecraft is

$$T = \frac{1}{2} \int_{m_S} |\dot{R}_S|^2 dm_S + \frac{1}{2} \int_{m_A} |\dot{R}_A|^2 dm_A$$

$$= \frac{1}{2} \int_{m_S} |\dot{R} + \omega \times c|^2 dm_S + \frac{1}{2} \int_{m_A} |\dot{R} + \omega \times (a + u) + \dot{u}|^2 dm_A$$

$$= \frac{1}{2} m |\dot{R}|^2 + \frac{1}{2} \omega^T I_0 \omega + \dot{R} \cdot (\omega \times S_0) + \frac{1}{2} \int_{m_A} |\dot{u}|^2 dm_A$$

$$+ \dot{R} \cdot [\int_{m_A} \dot{u} \, dm_A + \omega \times \int_{m_A} u \, dm_A] + \int_{m_A} \dot{u} \cdot (\omega \times a) dm_A$$

$$+ \int_{m_A} (\omega \times a) \cdot (\omega \times u) dm_A + \frac{1}{2} \int_{m_A} |\omega \times u|^2 dm_A$$

$$+ \int_{m_A} \dot{u} \cdot (\omega \times u) dm_A \tag{3}$$

where

$$S_0 = \int_{m_S} c \, dm_S + \int_{m_A} a \, dm_A \tag{4}$$

and m_S, m_A and m are the masses of the shuttle, the appendage and the entire spacecraft, respectively. Also, I_0 is the total mass moment of inertia matrix of the undeformed structure about point 0. Note that $|x|^2$ denotes the inner product $x \cdot x$.

The potential energy is due to the combined effects of gravity and strain energy. Assuming that the origin of the inertial coordinate system coincides with the center of the gravitational field, the gravitational potential can be expressed as

$$V_g = - Gm_e [\int_{m_S} |\underline{R} + \underline{r}|^{-1} dm_S + \int_{m_A} |\underline{R} + \underline{a} + \underline{u}|^{-1} dm_A]$$ (5)

where m_e is the mass of the earth and G is the universal gravitational constant.

The strain energy can be expressed as an energy inner product denoted by $[\ ,\ ]$ (Ref. 1). The total potential energy then becomes

$$V = \frac{1}{2}[\underline{u},\underline{u}] + V_g .$$ (6)

The virtual work is due to external forces, including control forces. Denoting by $\underline{f}_S$ the force vector per unit volume of the shuttle and by $\underline{f}_A$ the force vector per unit volume of the appendage, we can write the virtual work as

$$\delta W = \int_{D_S} \underline{f}_S \cdot \delta \underline{R}_S \ dD_S + \int_{D_A} \underline{f}_A \cdot \delta \underline{R}_A \ dD_A$$ (7)

where D_S and D_A are the domains of the shuttle and appendage, respectively.

Next, we propose to discretize the system in space. To this end, we express the elastic displacements in the form of linear combinations of admissible functions, or

$$\underline{u} = \phi q$$ (8)

where ϕ is a matrix of space-dependent admissible functions and q is a vector of time-dependent generalized coordinates. Introducing Eq. (8) into Eq. (3), the kinetic energy takes the matrix form

$$T = \frac{1}{2} m \dot{\underline{R}}^T \dot{\underline{R}} + \frac{1}{2} \underline{\omega}^T I_0 \underline{\omega} + \dot{\underline{R}}^T c^T \tilde{S}_0 \underline{\omega} + \frac{1}{2} \dot{q}^T M_A \dot{q} + \dot{\underline{R}}^T c^T \bar{\phi} \dot{q} + \dot{\underline{R}}^T c^T \tilde{\omega}^T \bar{\phi} q$$

$$+ \dot{q}^T \tilde{\phi}^T \underline{\omega} + \underline{\omega}^T \int_{m_A} \tilde{a}^T \tilde{\omega}^T \phi \ dm_A q - \frac{1}{2} q^T \bar{L}_A(\underline{\omega})q + \dot{q}^T L_A(\underline{\omega})q$$ (9)

where

$$\bar{\phi} = \int_{m_A} \phi \ dm_A, \quad \tilde{\phi}^T = \int_{m_A} \phi^T \tilde{a} \ dm_A$$ (10a,b)

$$L_A(\underline{\omega}) = \int_{m_A} \phi^T \tilde{\omega}^T \phi \ dm_A, \quad \bar{L}_A(\underline{\omega}) = \int_{m_A} \phi^T \tilde{\omega}^2 \phi \ dm_A$$ (10c,d)

and

$$M_A = \int_{m_A} \phi^T \phi \; dm_A \tag{10e}$$

is the mass matrix of the appendage. The symbol C represents a rotation matrix from the inertial frame XYZ to the $x_0 y_0 z_0$ frame and its elements are nonlinear functions of Euler's angles $\underline{\alpha}$. The tilde over a typical vector $\underline{v}$ denotes a skew symmetric matrix of the form

$$\tilde{v} = \begin{bmatrix} 0 & v_z & -v_y \\ -v_z & 0 & v_x \\ v_y & -v_x & 0 \end{bmatrix} \tag{11}$$

Recognizing that the magnitude of $\underline{R}$ is large and $\underline{u}$ is small in comparison with the other vectors in Eq. (5) and ignoring terms of order higher than three, a binomial expansion permits us to write

$$V_g \stackrel{\sim}{=} - Gm_e[m|\underline{R}|^{-1} - \underline{R} \cdot (\underline{S}_0 + \int_{m_A} \underline{u} \; dm_A)|\underline{R}|^{-3}] \tag{12}$$

Introducing Eq. (12) into Eq. (6) and considering Eq. (8), the potential energy can be written in the form

$$V = \frac{1}{2} \underline{g}^T K_A \underline{g} - \frac{Gm_e m}{|\underline{R}|} + \frac{Gm_e}{|\underline{R}|^3} \underline{R}^T C^T (\underline{S}_0 + \bar{\phi}q) \tag{13}$$

where

$$K_A = [\phi, \; \phi] \tag{14}$$

is the stiffness matrix of the appendage. The virtual work can be shown to have the expression

$$\delta W = \underline{F}^T C \delta \underline{R} + \underline{M}^T D(\underline{\alpha}) \delta \underline{\alpha} + \underline{Q}^T \delta \underline{g} \tag{15}$$

where

$$\underline{F} = \int_{D_S} \underline{f}_S \; dD_S + \int_{D_A} \underline{f}_A \; dD_A \tag{16a}$$

$$\underset{\sim}{M} = \int_{D_S} \tilde{r}^T \underset{\sim}{f}_S \, dD_S + \int_{D_A} \tilde{a}^T \underset{\sim}{f}_A \, dD_A + \int_{D_A} \tilde{f}_A \Phi \, dD_A \underset{\sim}{q} \tag{16b}$$

$$\underset{\sim}{Q} = \int_{D_A} \Phi^T \underset{\sim}{f}_A \, dD_A \tag{16c}$$

are generalized force vectors in terms of components about x_0, y_0 and z_0 and $D(\underset{\sim}{\alpha})$ is a matrix of trigonometric functions of the Euler angles defined by the expression

$$\underset{\sim}{\omega} = D(\underset{\sim}{\alpha})\dot{\underset{\sim}{\alpha}} \tag{16a}$$

Lagrange's equations of motion can be written in the symbolic form

$$\frac{d}{dt}\left(\frac{\partial T}{\partial \dot{\underset{\sim}{R}}}\right) + \frac{\partial V}{\partial \underset{\sim}{R}} = C^T \underset{\sim}{F} \tag{17a}$$

$$\frac{d}{dt}\left(\frac{\partial T}{\partial \dot{\underset{\sim}{\alpha}}}\right) - \frac{\partial T}{\partial \underset{\sim}{\alpha}} + \frac{\partial V}{\partial \underset{\sim}{\alpha}} = D^T \underset{\sim}{M} \tag{17b}$$

$$\frac{d}{dt}\left(\frac{\partial T}{\partial \dot{\underset{\sim}{q}}}\right) - \frac{\partial T}{\partial \underset{\sim}{q}} + \frac{\partial V}{\partial \underset{\sim}{q}} = \underset{\sim}{Q} \tag{17c}$$

so that, considering Eqs. (9), (13) and (15) and premultiplying Eq. (17b) by D^{-T}, the equations of motion for the spacecraft in orbit are

$$m\ddot{\underset{\sim}{R}} + C^T \tilde{S}_0 \dot{\underset{\sim}{\omega}} + C^T \overline{\Phi}\ddot{\underset{\sim}{q}} + C^T \tilde{\omega}^T \tilde{S}_0 \underset{\sim}{\omega} + 2C^T \tilde{\omega}^T \overline{\Phi}\dot{\underset{\sim}{q}} + C^T(\tilde{\omega}^2 + \dot{\tilde{\omega}}^T)\overline{\Phi}\underset{\sim}{q}$$

$$+ \frac{Gm_e}{|\underset{\sim}{R}|^3}\{m\underset{\sim}{R} + C^T(\underset{\sim}{S}_0 + \overline{\Phi}\underset{\sim}{q}) - 3[\hat{\underset{\sim}{R}}\,\hat{\underset{\sim}{R}}^T C^T(\underset{\sim}{S}_0 + \overline{\Phi}\underset{\sim}{q})]\} = C^T \underset{\sim}{F} \tag{18a}$$

$$I_0 \dot{\underset{\sim}{\omega}} + \tilde{\omega}^T I_0 \underset{\sim}{\omega} + \tilde{S}_0^T C\ddot{\underset{\sim}{R}} + \overline{\Phi}\ddot{\underset{\sim}{q}} + [\widetilde{[CR]}\overline{\Phi} + J(\dot{\underset{\sim}{\omega}}) + \tilde{\omega}^T J(\underset{\sim}{\omega}) + \frac{Gm_e}{|\underset{\sim}{R}|^3}\widetilde{[CR]}\overline{\Phi}]\underset{\sim}{q}$$

$$+ [\tilde{\omega}^T \overline{\Phi} + J(\omega)]\dot{\underset{\sim}{q}} + \frac{Gm_e}{|\underset{\sim}{R}|^3}\widetilde{[CR]}\underset{\sim}{S}_0 = \underset{\sim}{M} \tag{18b}$$

$$M_A \ddot{\underset{\sim}{q}} + \overline{\Phi}^T C\ddot{\underset{\sim}{R}} + \overline{\Phi}^T \dot{\underset{\sim}{\omega}} + \int_{m_A} \Phi^T \tilde{\omega}^T \tilde{a}_0 \, dm_A + \frac{Gm_e}{|\underset{\sim}{R}|^3}\overline{\Phi}^T C\underset{\sim}{R}$$

$$+ \tilde{L}_A(\omega)\dot{\underset{\sim}{q}} + [\tilde{L}_A(\omega) + L_A(\dot{\underset{\sim}{\omega}}) + K_A]\underset{\sim}{q} = \underset{\sim}{Q} \tag{18c}$$

where

$$J(\underline{\omega}) = \int_{m_A} (\tilde{a}\tilde{\omega} + \widetilde{[\tilde{a}\underline{\omega}]})\phi \ dm_A \tag{18d}$$

and

$$\hat{\underline{R}} = \frac{\underline{R}}{|\underline{R}|} \tag{18e}$$

Premultiplying Eq. (17b) by D^{-T} is equivalent to considering Lagrange's equations in terms of quasi-coordinates (Ref. 2). Note that the position vector $\underline{R}$, its time derivatives, and the Euler angles $\underline{y}$ have been considered to be of arbitrary magnitude, with the result that many nonlinear terms appear in Eqs. (18).

3. Equations of Motion for the Laboratory Experiment

In the laboratory experiment, the spacecraft is not actually free in space, but suspended from the ceiling by means of a cable or a beam. The following analysis applies to either case. The support is likely to affect the dynamic characteristics of the system. Hence, in the sequel, the support is added to the free model in the form of an elastic member.

Considering Fig. 2, the position vector for an arbitrary point C on the cable is $\underline{R}_C = \underline{c} + \underline{w}$, where $\underline{c}$ is a position vector and $\underline{w}$ is the elastic displacement of the cable, both of which are measured with respect to the inertial frame. The position vector for the point 0 is

$$\underline{R} = \underline{c}_B + \underline{w}_B + \underline{e} \tag{19}$$

where the subscript B denotes evaluation at the point B and $\underline{e}$ is the vector from point B (ball joint) to the point 0 fixed on the shuttle, measured with respect to the $x_0 y_0 z_0$ frame. The velocity vector of an arbitrary point C on the cable is then

$$\dot{\underline{R}}_C = \dot{\underline{w}} \tag{20}$$

and the velocity of point 0 is

$$\dot{\underline{R}} = \dot{\underline{w}}_B + \underline{\omega} \times \underline{e} \tag{21}$$

The kinematics for the shuttle body and appendage remain the same as for the unrestrained spacecraft in space. Hence, the kinetic energy for the entire structure is

$$
\begin{aligned}
T &= \frac{1}{2} \int_{m_C} |\dot{R}_C|^2 dm_C + \frac{1}{2} \int_{m_S} |\dot{R}_S|^2 dm_S + \frac{1}{2} \int_{m_A} |\dot{R}_A|^2 dm_A \\
&= \frac{1}{2} \int_{m_C} |\dot{w}|^2 dm_C + \frac{1}{2} \int_{m_S} |\dot{w}_B + \underline{\omega} \times (\underline{e} + \underline{c})|^2 dm_S \\
&\quad + \frac{1}{2} \int_{m_A} |\dot{w}_B + \underline{\omega} \times (\underline{e} + \underline{a} + \underline{u}) + \dot{\underline{u}}|^2 dm_A \\
&= \frac{1}{2} \int_{m_C} |\dot{w}|^2 dm_C + \frac{1}{2} m |\dot{w}_B|^2 + \frac{1}{2} \underline{\omega}^T I_0 \underline{\omega} + \frac{1}{2} m (\underline{\omega} \times \underline{e}) \cdot (\underline{\omega} \times \underline{e}) \\
&\quad + \dot{w}_B \cdot (\underline{\omega} \times \underline{S}_B) + (\underline{\omega} \times \underline{e}) \cdot (\underline{\omega} \times \underline{S}_0) + \frac{1}{2} \int_{m_A} |\dot{u}|^2 dm_A \\
&\quad + \dot{w}_B \cdot \int_{m_A} \dot{\underline{u}} \, dm_A + \int_{m_A} \dot{\underline{u}} \cdot (\underline{\omega} \times \underline{b}) dm_A + \int_{m_A} (\underline{\omega} \times \underline{b}) \cdot (\underline{\omega} \times \underline{u}) \, dm_A \\
&\quad + \frac{1}{2} \int_{m_A} |\underline{\omega} \times \underline{u}|^2 \, dm_A + \int_{m_A} \dot{\underline{u}} \cdot (\underline{\omega} \times \underline{u}) \, dm_A
\end{aligned}
\tag{22}
$$

where

$$
\underline{S}_B = \underline{S}_0 + m\underline{e}, \quad \underline{b} = \underline{a} + \underline{e}
\tag{23}
$$

The elastic displacement vectors $\underline{u}$ and $\underline{w}$ have been assumed to be small.

The expression for the virtual work is given by Eq. (7), but the potential energy must be modified. The acceleration of gravity will be assumed to be constant and can be expressed as $\underline{g} = -g\underline{u}_Z$ so that the gravitational potential is

$$
V_g = \int_{m_C} (\underline{c} + \underline{w}) \cdot \underline{g} \, dm_C + \int_{m_S} (\underline{R} + \underline{c}) \cdot \underline{g} \, dm_S + \int_{m_A} (\underline{R} + \underline{a} + \underline{u}) \cdot \underline{g} \, dm_A
\tag{24}
$$

where $\underline{R}$ is defined by Eq. (19) and $\underline{u}_Z$ is a unit vector in the Z direction. The elastic potential energy for the system can be expressed as

$$
V_E = \frac{1}{2} [\underline{u}, \underline{u}] + \frac{1}{2} [\underline{w}, \underline{w}]
\tag{25}
$$

where $[\underline{w}, \underline{w}]$ is the energy inner product for the cable, which includes a

stiffening effect due to the weight of the spacecraft model. Because a cable has little inherent bending stiffness, the stiffening effect can be significant.

As with the appendage in the preceding section, the elastic displacement of the cable can be approximated by a linear combination of admissible functions, or

$$\underline{w} = \psi \underline{q} \tag{26}$$

where ψ is a matrix of space-dependent admissible functions and $\underline{q}$ is a vector of time-dependent generalized coordinates. Introducing Eqs. (8) and (26) into Eq. (22), the kinetic energy takes the matrix form

$$T = \frac{1}{2}\dot{\underline{q}}^T M_C \dot{\underline{q}} + \frac{1}{2}\underline{\omega}^T (I_0 + m\tilde{e}^T\tilde{e} + 2\tilde{e}^T S_0)\underline{\omega} + \dot{\underline{q}}^T \psi_B^T C^T \tilde{S}_B \underline{\omega} + \frac{1}{2}\dot{\underline{q}}^T M_A \dot{\underline{q}}$$

$$+ \dot{\underline{q}}^T \psi_B^T C^T \overrightarrow{\psi q} + \dot{\underline{q}}^T \psi_B^T C^T \tilde{\omega}^T \overrightarrow{\psi q} + \dot{\underline{q}}^T \tilde{q} I_\omega$$

$$+ \underline{\omega}^T \int_{m_A} \tilde{b}\tilde{\omega}\phi \, dm_A \, \underline{q} + \dot{\underline{q}}^T \tilde{L}_A(\underline{\omega})\underline{q} - \frac{1}{2}\underline{q}^T \tilde{L}_A(\underline{\omega})\underline{q} \tag{27a}$$

where

$$\tilde{\psi}^T = \int_{m_A} \phi^T \tilde{b} \, dm_A \tag{27b}$$

has been redefined and

$$M_C = \int_{m_C} \psi^T \psi \, dm_C + m\psi_B^T \psi_B \tag{27c}$$

is the combined mass matrix of the cable and of the structure lumped at the end of the cable, in which ψ_B denotes the matrix ψ evaluated at B. Introducing Eqs. (8) and (26) into Eqs. (24) and (25) the potential energy can be written in the matrix form

$$V = \underline{q}^T \overline{\psi} \underline{g} + S_B^T C \underline{g} + m\underline{q}^T \psi_B^T \underline{g} + \underline{g}^T \overline{\psi}^T C \underline{g} + \frac{1}{2}\underline{g}^T K_A \underline{g} + \frac{1}{2}\underline{q}^T K_C \underline{q} \tag{28}$$

where

$$\overline{\psi} = \int_{m_C} \psi \, dm_C \tag{29a}$$

and

$$K_C = [\psi, \psi] \tag{29b}$$

is the stiffness matrix of the support. Considering Eqs. (19) and (25), the virtual work can be expressed as

$$\delta W = F^T C \psi_B \delta \eta + M^T D(\alpha) \delta \alpha + Q^T \delta y \tag{30}$$

where all the terms have been defined previously. The effect of the friction of the ball joint can be assumed in the form of an external torque. Hence, we let $M = M_c + M_f$ in Eq. (30), where M_c is a vector of control moments and M_f is a vector of frictional moments caused by the ball joint.

Lagrange's equations remain in the symbolic form of Eqs. (17), with the exception of Eq. (17a) which must be replaced by

$$\frac{d}{dt}\left(\frac{\partial T}{\partial \dot{\eta}}\right) + \frac{\partial V}{\partial \eta} = \psi_B^T C^T F \tag{32}$$

Using the same approach as in Sec. 2, the equations of motion for the laboratory experiment can be shown to have the form

$$M_C \ddot{\eta} + \psi_B^T C^T \tilde{S}_B \dot{\omega} + \psi_B^T C^T \tilde{\omega}^T \tilde{S}_B \omega + \psi_B^T C^T \bar{\Phi} \ddot{y} + 2\psi_B^T C^T \tilde{\omega}^T \bar{\Phi} \dot{y}$$

$$+ \psi_B^T C^T (\tilde{\omega}^2 + \dot{\tilde{\omega}}^T) \bar{\Phi} y + (m\psi_B^T + \bar{\Psi}^T) y + K_C \eta = \psi_B^T C^T F \tag{33a}$$

$$I_B \dot{\omega} + \tilde{\omega}^T I_B \omega + \tilde{S}_B^T C \psi_B \ddot{\eta} + \tilde{\Phi} \ddot{q} + [J(\dot{\omega}) + \tilde{\omega}^T J(\omega)$$

$$+ [\widetilde{Cy}] \bar{\Psi}] y + [\tilde{\omega}^T \tilde{\Phi} + J(\omega)] \dot{y} + [\widetilde{Cy}] S_B = M \tag{33b}$$

$$M_A \ddot{y} + \bar{\Phi}^T C \psi_B \ddot{\eta} + \tilde{\Phi}^T \dot{\omega} + \int_{m_A} \phi^T \tilde{\omega}^T \tilde{b}_\omega \, dm_A$$

$$+ \bar{\Phi}^T C y + \tilde{L}_A(\omega) \dot{y} + [\bar{L}_A(\omega) + \dot{L}_A(\omega) + K_A] y = Q \tag{33c}$$

where $J(\omega)$ is redefined by replacing a with b in Eq. (18d) and

$$I_B = I_0 + m\tilde{e}^T\tilde{c} + \tilde{e}^T\tilde{S}_0 + \tilde{S}_0^T\tilde{e} \tag{33d}$$

is the mass moment of inertia of the spacecraft about point B. In this case, the set of Euler angles $\underset{\sim}{\alpha}$ is assumed to be of arbitrary magnitude, which is responsible for many nonlinear terms in Eqs. (33).

4. Simulation and Control

The nonlinear equations of motion for the orbiting spacecraft have the same basic form as for the laboratory experiment. Hence, the approach to the solution suggested here applies for both situations.

Consider a first-order perturbation on the quantities $\underset{\sim}{R}$ and $\underset{\sim}{\alpha}$.

$$\underset{\sim}{R} = \underset{\sim}{R}_0 + \underset{\sim}{R}_1 \ , \quad \underset{\sim}{\alpha} = \underset{\sim}{\alpha}_0 + \underset{\sim}{\alpha}_1 \tag{34a,b}$$

where the first order terms $\underset{\sim}{R}_1$ and $\underset{\sim}{\alpha}_1$ are small compared to the zero order terms $\underset{\sim}{R}_0$ and $\underset{\sim}{\alpha}_0$. Introducing Eqs. (34) into the nonlinear equations of motion, Eqs. (18) or (33), and separating orders of magnitudes, we obtain zero-order and first-order perturbation equations. The zero-order equations can be used for the maneuvering of the spacecraft and the first-order equations for vibration suppression and rigid-body corrections. Before proceeding with this technique, we will first develop some expressions relating the perturbations in the Euler angles, $\underset{\sim}{\alpha}$, with small angular deflections, $\underset{\sim}{\beta}$, expressed in the body-fixed frame. This is done so that all the variables in the perturbation equations can be expressed in the body-fixed frame, the frame in which state measurements will be taken and actuating forces will be applied. Note that a set of Euler angles of arbitrary magnitude do not form a vector whereas the angles $\underset{\sim}{\beta}$, being small, can be thought of as a vector quantity.

First consider Eq. (16a) which relates the velocities of the Euler angles to the body fixed angular velocities, $\underset{\sim}{\omega}$. Introducing Eq. (34b) into Eq. (16a) and neglecting higher-order terms, we obtain the perturbed angular velocity vector

$$\underset{\sim}{\omega} = \underset{\sim}{\omega}_0 + \underset{\sim}{\omega}_1 \tag{35}$$

where

$$\omega_0 = D(\alpha_0)\dot{\alpha}_0 \ , \quad \omega_1 = D(\alpha_1)\dot{\alpha}_0 + D(\alpha_0)\dot{\alpha}_1 \qquad (36a,b)$$

Using similar considerations, it can be shown that the body-fixed perturbation angles can be related to the perturbed Euler angles by the expression

$$\beta = D(\alpha_0)\alpha_1 \qquad (37)$$

Note that the vector β is a first-order perturbation of a set of quasi-coordinates (Ref. 2). Taking the time derivative of Eq. (37) and introducing into Eq. (36b), the perturbed angular velocity vector, ω_1, is related to the angles β by the expression

$$\omega_1 = \tilde{\omega}_0^T \beta + \dot{\beta} \qquad (38)$$

Taking the time derivative of Eq. (38), the perturbed angular acceleration becomes

$$\dot{\omega}_1 = \dot{\tilde{\omega}}_0^T \beta + \tilde{\omega}_0^T \dot{\beta} + \ddot{\beta} \qquad (39)$$

Recall that the elements of the transformation matrix C from the body-fixed frame to the inertial frame consist of trigonometric functions of the Euler angles, so that a perturbation of this matrix will also involve the vector β. This relation can be derived using Eq. (37). Instead, consider the frame O' which differs from the O frame by the angles β. Then, the transformation from the O' frame to the O frame is $[I + \tilde{\beta}]$ where I is an identity matrix. Letting C_0 be the transformation matrix from the O frame to the inertial frame, the total transformation matrix, C, from the O' frame to the inertial frame can be expressed as

$$C = C_0 + C_1 \qquad (40)$$

where

$$C_1 = \tilde{\beta} C_0 \qquad (41)$$

In keeping with our objective of expressing the first-order perturbation

equations in the body fixed frame, Eq. (34a) is replaced by

$$R = R_0 + c_0^T R_1 \tag{42}$$

where R_1 is now a vector measured with respect to the 0 frame. The control forces and moments can also be expressed in first-order . perturbed form as follows:

$$E = E_0 + E_1 \quad , \quad M = M_0 + M_1 \tag{43a,b}$$

Introducing Eqs. (34) through (43) into Eqs. (18) and neglecting higher-order terms, we obtain two sets of equations of motion for the spacecraft in orbit. The zero-order equations, which govern the motion of the structure as if it were rigid, can be expressed as

$$m\ddot{R}_0 + c_0^T \tilde{S}_0 \dot{\omega}_0 + c_0^T \tilde{\omega}_0 \tilde{S}_0 \omega_0 + \frac{Gm_e}{|R_0|^3} [m R_0 + (I - 3\hat{R}_0 \hat{R}_0^T) c_0^T S_0] = c_0^T E_0 \tag{44a}$$

$$\tilde{S}_0^T c_0 \ddot{R}_0 + \frac{Gm_e}{|R_0|^3} \tilde{S}_0^T c_0 R_0 + I_0 \dot{\omega}_0 + \tilde{\omega}_0^T I_0 \omega_0 = M_0 \tag{44b}$$

The first-order equations, which govern the small scale motions of the structure, can be expressed as

$$m\ddot{R}_1 + 2m\tilde{\omega}_0^T \dot{R}_1 + [\dot{\tilde{\omega}}_0^T + \tilde{\omega}_0^2 + \Pi] R_1 + \tilde{S}_0 \ddot{\beta} + 2\tilde{\omega}_0^T \tilde{S}_0 \dot{\beta} + [\dot{\tilde{\omega}}_0^T + \tilde{\omega}_0^2 + \Pi] \tilde{S}_0 \beta$$

$$+ \tilde{F}_0^T \beta + \overline{\phi} \ddot{q} + 2\tilde{\omega}_0^T \overline{\phi} \dot{q} + [\dot{\tilde{\omega}}_0^T + \tilde{\omega}_0^2 + \Pi] \overline{\phi} q = F_1 \tag{45a}$$

$$\tilde{S}_0^T \ddot{R}_1 + 2\tilde{S}_0^T \tilde{\omega}_0^T \dot{R}_1 + \tilde{S}_0^T [\dot{\tilde{\omega}}_0^T + \tilde{\omega}_0^2 + \Pi] R_1 + \tilde{F}_0 R_1$$

$$+ I_0 \ddot{\beta} + [I\dot{\tilde{\omega}}_0^T + \tilde{\omega}_0^T I_0 + \widetilde{[I_0 \omega_0]}] \dot{\beta}$$

$$+ [I_0 \dot{\tilde{\omega}}_0^T + \tilde{\omega}_0^T I_0 \tilde{\omega}_0^T + \widetilde{[I_0 \omega_0]} \tilde{\omega}_0^T + \tilde{S}_0 H] \beta + \overline{\phi} \ddot{q}$$

$$+ [\tilde{\omega}_0^T \overline{\phi} + J_0] \dot{q} + [\dot{J}_0 + \tilde{\omega}_0^T J_0 + H\overline{\phi}] q = M_1 \tag{45b}$$

$$\overline{\phi}^T \ddot{R}_1 + 2\overline{\phi}^T \tilde{\omega}_0^T \dot{R}_1 + \overline{\phi}^T [\dot{\tilde{\omega}}_0^T + \tilde{\omega}_0^2 + \Pi] R_1 + \tilde{\phi}^T \ddot{\beta}$$

$$+ [\tilde{\phi}^T\tilde{\omega}_0^T - J_0^T]\dot{\underline{\beta}} + [\tilde{\phi}^T\dot{\tilde{\omega}}_0^T - J_0^T\tilde{\omega}_0^T + \overline{\phi}^T\tilde{H}]\underline{\beta}$$

$$+ M_A\ddot{\underline{g}} + \tilde{L}_A\dot{\underline{g}} + [\overline{L}_A + \dot{L}_A + K_A]\underline{g} = \underline{Q}_0 + \underline{Q}_1 \tag{45c}$$

where

$$\overline{H} = \frac{Gm_e}{|\underline{R}_0|^3} [I - 3C_0\hat{\underline{R}}_0\hat{\underline{R}}_0^T C_0^T] \tag{45d}$$

$$\tilde{H} = [\widetilde{C_0\ddot{\underline{R}}_0}] + \frac{Gm_e}{|\underline{R}_0|^3} [\widetilde{C_0\underline{R}_0}] \tag{45e}$$

$$\underline{Q}_0 = - [\overline{\phi}^T C_0\ddot{\underline{R}}_0 + \frac{Gm_e}{|\underline{R}_0|^3} \overline{\phi}^T C_0\underline{R}_0 + \tilde{\phi}^T\dot{\underline{\omega}}_0 + \int_{m_A} \phi^T\tilde{\omega}_0^T\tilde{a}\underline{\omega}_0 \, dm_A] \tag{45f}$$

For the laboratory experiment to be successful, the deflections of the cable (translation of the spacecraft) should be small. From purely rigid-body dynamic considerations, the point B (ball joint) must be close to the center of mass in the direction normal to the axis of rotation during a maneuver. Hence, the vector $\underline{S}_B$ can be considered to be small in the following analysis. Because the motion of the cable has been assumed to be small, introducing Eq. (36) into Eq. (33b), the z — order equations for the laboratory experiment are simply

$$\overline{I}_B\dot{\underline{\omega}}_0 + \tilde{\omega}_0^T I_B\underline{\omega}_0 = \underline{M}_0 \tag{46}$$

The motion of the cable, $\psi\underline{\eta}$, can be expressed with respect to the body-fixed frame, as was done with the vector $\underline{R}_1$ for the orbiting spacecraft. Introducing Eqs. (36), (39), (40), (41) and (43) into Eqs. (33) and neglecting higher-order terms, the first-order equations of motion for the laboratory experiment can be expressed as follows:

$$M_C\ddot{\underline{\eta}} + 2\tilde{L}_C\dot{\underline{\eta}} + [\dot{L}_C + \overline{L}_C + K_C]\underline{\eta} + \psi_B^T\tilde{S}_B\ddot{\underline{\beta}} + 2\psi_B^T\tilde{\omega}_0^T\tilde{S}_B\dot{\underline{\beta}} + \psi_B^T[\dot{\tilde{\omega}}_0^T + \tilde{\omega}_0^2]\tilde{S}_B\underline{\beta}$$

$$+ \psi_B^T\overline{\phi}\ddot{\underline{g}} + 2\psi_B^T\tilde{\omega}_0^T\overline{\phi}\dot{\underline{g}} + \psi_B^T[\dot{\tilde{\omega}}_0^T + \tilde{\omega}_0^2]\overline{\phi}\underline{g} = \underline{E}_0 + \psi_B^T\underline{E} \tag{47a}$$

$$\tilde{S}_B^T\psi_B\ddot{\underline{\eta}} + 2\tilde{S}_B^T\tilde{\omega}_0^T\psi_B\dot{\underline{\eta}} + \tilde{S}_B^T[\dot{\tilde{\omega}}_0^T + \tilde{\omega}_0^2]\psi_B\underline{\eta}$$

$$+ I_B \ddot{\beta} + [I_B \tilde{\omega}_0^T + \tilde{\omega}_0^T I_B + [\widetilde{I_B \tilde{\omega}_0}]]\dot{\beta}$$

$$+ [I_B \dot{\tilde{\omega}}_0^T + \tilde{\omega}_0^T I_B \tilde{\omega}_0^T + [\widetilde{I_B \tilde{\omega}_0}]\tilde{\omega}_0^T + \tilde{S}_B[\widetilde{C_0 g}]]\beta$$

$$+ \tilde{\Phi} \ddot{g} + [\tilde{\omega}_0^T \tilde{\Phi} + J_0]\dot{g} + [\dot{J}_0 + \tilde{\omega}_0^T J_0 + [\widetilde{C_0 g}]\tilde{\Phi}]g$$

$$= M_0 + M_0' + M_1 \tag{47b}$$

$$\tilde{\Phi}^T \psi_B \ddot{\eta} + 2\tilde{\Phi}^T \tilde{\omega}_0^T \psi_B \dot{\eta} + \tilde{\Phi}^T (\dot{\tilde{\omega}}_0^T + \tilde{\omega}_0^2)\psi_B \eta$$

$$+ \tilde{\Phi}^T \ddot{\beta} + [\tilde{\Phi}^T \tilde{\omega}_0^T - J_0^T]\dot{\beta} + [\tilde{\Phi}^T \dot{\tilde{\omega}}_0^T - J_0^T \tilde{\omega}_0^T + \tilde{\Phi}^T[\widetilde{C_0 g}]^T]\beta$$

$$+ M_A \ddot{g} + \tilde{L}_A \dot{g} + [\tilde{L}_A + \dot{L}_A + K_A]g = g_0 + g_1 \tag{47c}$$

where

$$E_0 = - \psi_B^T [\tilde{\omega}_0^T \tilde{S}_B \tilde{\omega}_0 + \tilde{S}_B \dot{\tilde{\omega}}_0] - (m\psi_B^T + \tilde{\Phi}^T)C_0 g \tag{47d}$$

$$M_0' = \tilde{S}_B C_0 g \tag{47e}$$

$$g_0 = - [\tilde{\Phi}^T \dot{\tilde{\omega}}_0 + \int_{m_A} \Phi^T \tilde{\omega}_0^T \tilde{b} \tilde{\omega}_0 \, dm_A + \tilde{\Phi}^T C_0 g] \tag{47f}$$

For the orbiting spacecraft, Eqs. (44) can be solved for $E_0(t)$ and $M_0(t)$ for any desired maneuver strategy $R_0(t)$ and $\omega_0(t)$. For the laboratory experiment, Eqs. (46) can be solved for $M_0(t)$ for any desired $\omega_0(t)$. In either case, these quantities can then be substituted into the first-order equations (Eqs. (45) or (47)) producing a set of linear equations with known time-varying coefficients which govern the small deviations from the rigid-body maneuver and elastic motions of the structure. These linear equations can be expressed in the matrix form

$$M\ddot{x} + G\dot{x} + (K_S + K_{NS})x = E^* \tag{48}$$

where for the orbiting case

$$x^T = [R_1^T \quad \beta^T \quad g^T] \tag{49a}$$

$$\underset{\sim}{E}^{*T} = [E_1^T \quad M_1^T \quad g_0^T + g_1^T] \tag{49b}$$

$$M = \begin{bmatrix} M_0 & \tilde{S}_0 & \bar{\Phi} \\ \tilde{S}_0^T & I_0 & \tilde{\Phi} \\ \bar{\Phi}^T & \tilde{\Phi}^T & M_\Lambda \end{bmatrix} \qquad M_0 = \begin{bmatrix} m & 0 & 0 \\ 0 & m & 0 \\ 0 & 0 & m \end{bmatrix} \tag{49c,d}$$

$$G = \begin{bmatrix} 2M_0\tilde{\omega}_0^T & 2\tilde{\omega}_0^T\tilde{S}_0 & 2\tilde{\omega}_0^T\tilde{\Phi} \\ -2(\tilde{\omega}_0^T\tilde{S}_0)^T & I_0\tilde{\omega}_0^T + \tilde{\omega}_0^T I_0 + [\widetilde{I_0\tilde{\omega}_0}] & \tilde{\omega}_0^T\tilde{\Phi} + J_0 \\ -2(\tilde{\omega}_0^T\bar{\Phi})^T & -[\tilde{\omega}_0^T\tilde{\Phi} + J_0]^T & 2\tilde{L}_A \end{bmatrix} \tag{49e}$$

$$K_s = \begin{bmatrix} M_0[\tilde{\omega}_0^2 + \bar{H}] & \tilde{F}_0^T + [\tilde{\omega}_0^2 + \bar{H}]\tilde{S}_0 & [\tilde{\omega}_0^2 + \bar{H}]\bar{\Phi} \\ \tilde{F}_0 + \tilde{S}_0^T[\tilde{\omega}_0^2 + \bar{H}] & \tilde{\omega}_0 I_0 \tilde{\omega}_0 & \tilde{\omega}_0^T J_0 + \tilde{H}\tilde{\Phi} \\ \bar{\Phi}^T[\tilde{\omega}_0^2 + \bar{H}] & J_0^T\tilde{\omega}_0 + \bar{\Phi}^T\tilde{H}^T & \bar{L}_A + K_A \end{bmatrix} \tag{49f}$$

$$K_{NS} = \begin{bmatrix} M_0\dot{\tilde{\omega}}_0^T & \dot{\tilde{\omega}}_0^T\tilde{S}_0 & \dot{\tilde{\omega}}_0^T\bar{\Phi} \\ -(\dot{\tilde{\omega}}_0^T\tilde{S}_0)^T & I_0\dot{\tilde{\omega}}_0^T + [\widetilde{I_0\tilde{\omega}_0}]\tilde{\omega}_0^T + \tilde{S}_0 H & \dot{J}_0 \\ -(\dot{\tilde{\omega}}_0^T\bar{\Phi})^T & \tilde{\Phi}^T\dot{\tilde{\omega}}_0^T & \dot{\tilde{L}}_A \end{bmatrix} \tag{49g}$$

and for the laboratory experiment

$$\underset{\sim}{x}^T = [q^T \quad \dot{q}^T \quad g^T] \tag{50a}$$

$$\underset{\sim}{E}^{*T} = [E_0^T + \psi_B E_1^T \quad M_0'^T + M_1^T \quad g_0^T + g_1^T] \tag{50b}$$

$$M = \begin{bmatrix} M_C & \psi_B^T\tilde{S}_B & \psi_B^T\bar{\Phi} \\ \tilde{S}_B^T\psi_B & I_B & \tilde{\Phi} \\ \bar{\Phi}^T\psi_B & \tilde{\Phi}^T & M_A \end{bmatrix} \tag{50c}$$

$$G = \begin{bmatrix} 2\tilde{L}_C & 2\psi_B^T\tilde{\omega}_0^T\tilde{S}_B & 2\psi_B^T\tilde{\omega}_0^T\overline{\phi} \\ -2(\psi_B^T\tilde{\omega}_0^T\tilde{S}_B)^T & I_B\tilde{\omega}_0^T + \tilde{\omega}_0^T I_B + [\widetilde{I_B\tilde{\omega}_0}] & \tilde{\omega}_0^T\overline{\phi} + J_0 \\ -2(\psi_B^T\tilde{\omega}_0^T\overline{\phi}) & -[\tilde{\omega}_0^T\overline{\phi} + J_0]^T & 2\tilde{L}_A \end{bmatrix} \tag{50d}$$

$$K_S = \begin{bmatrix} \overline{L}_C + K_C & \psi_B^T\tilde{\omega}_0^2\tilde{S}_B & \psi_B^T\tilde{\omega}_0^2\overline{\phi} \\ \tilde{S}_B^T\tilde{\omega}_0^2\psi_B & \tilde{\omega}_0 I_B\tilde{\omega}_0 & \tilde{\omega}_0^T J_0 + [\widetilde{C_0 g}]\overline{\phi} \\ \overline{\phi}^T\tilde{\omega}_0^2\psi_B & J_0^T\tilde{\omega}_0 + \overline{\phi}^T[\widetilde{C_0 g}]^T & \overline{L}_A + K_A \end{bmatrix} \tag{50e}$$

$$K_{NS} = \begin{bmatrix} \dot{\tilde{L}}_C & \psi_B^T\dot{\tilde{\omega}}_0^T\tilde{S}_B & \psi_B^T\dot{\tilde{\omega}}_0^T\overline{\phi} \\ -(\psi_B^T\dot{\tilde{\omega}}_0^T\tilde{S}_B)^T & I_B\dot{\tilde{\omega}}_0^T + [\widetilde{I_B\tilde{\omega}_0}]\dot{\tilde{\omega}}_0^T + \tilde{S}_B[\widetilde{C_0 g}] & \dot{J}_0 \\ -(\psi_B^T\dot{\tilde{\omega}}_0^T\overline{\phi})^T & \overline{\phi}^T\dot{\tilde{\omega}}_0^T & \dot{\tilde{L}}_A \end{bmatrix} \tag{50f}$$

In both cases, the mass matrix is symmetric. However, for the orbiting structure, the mass matrix is time invariant, whereas for the laboratory configuration, it is not. This is the case because the mass matrix of the cable, M_C, must be calculated with respect to the body-fixed frame, and hence it is a function of the transformation matrix $C_0(t)$. However, M_C and hence M can be considered time invariant if the axis of rotation is the axis of symmetry of the cable. In both cases, the time varying matrix G, multiplying the velocity vector, is skew-symmetric. This matrix contains the Coriolis (gyroscopic) terms.

The stiffness matrix has been split into two parts, one part, K_S, with purely symmetric terms, the other, K_{NS}, with the terms which lead to nonsymmetries. Of course, K_{NS} can be separated into symmetric and skew-symmetric matrices if desired. As can be seen in Eqs. (49g) and (50f), the terms containing the angular acceleration, $\dot{\omega}_0$, of the body-fixed frame lead to nonsymmetric terms in the stiffness matrix. In fact, many of these terms are skew-symmetric, and hence, circulatory. Note that the perturbation of the Euler equations resulted in some nonsymmetric terms containing only the angular velocity vector ω_0. This is not surprising, because it is well known that a steady-state rigid-body rotation about the axis of intermediate inertia is unstable. Owing to the nonsymmetry of the stiffness matrices, the vibration problem is non-self-adjoint in both cases.

Because we ignored structural damping, the matrix G was found to be purely gyroscopic, and hence conservative. However, the stiffness matrix was found to contain circulatory, nonconservative terms. Hence, during a rotation, the structure may be vibrating about an unstable equilibrium state, requiring active vibration control to stabilize the desired maneuver.

Gravity has a much stronger influence on the laboratory experiment, both because the force of gravity is greater, and because the opposing force is a point (cable) force rather than a body (centrifugal) force as with the orbiting structure. Hence, the static elastic displacement of the structure must be considered in determining the stable equilibrium orientation. It has been previously assumed that the ball joint is in the vicinity of the rigid-body center of mass along the axes orthogonal to the cable. That is, point B is near the center of mass, or perhaps somewhere above it. We now wish to find the stable equilibrium orientation and elastic deflection of the structure for a given ball joint location. For the laboratory experiment, the static portions of Eqs. (48) can be expressed as

$$K_{ST} x_{ST} = E_{ST} \tag{51}$$

where the static stiffness is

$$K_{ST} = \begin{bmatrix} K_C & 0 & 0 \\ 0 & \tilde{S}_B[\widetilde{C_0 g}] & [\widetilde{C_0 g}]\bar{\Phi} \\ 0 & \bar{\Phi}^T[\widetilde{C_0 g}]^T & K_A \end{bmatrix} \tag{51a}$$

and the static force is

$$E_{ST} = \begin{bmatrix} -(m\psi_B^T + \bar{\Phi}^T)C_0 g \\ \tilde{S}_B C_0 g \\ -\bar{\Phi}^T C_0 g \end{bmatrix} \tag{51b}$$

Equations (51) form a set of nonlinear algebraic equations which can be solved for x_{ST}, the static equilibrium orientation and elastic deflection of the structure. The elastic deflection is coupled with the angular orientation of the structure. Hence, the true center of mass depends on the orientation. The orientation about the longitudinal axis of the cable (direction of gravity) is arbitrary. This means that a

rotation about this axis will not affect the static orientation or elastic deflections. Any orientation can be made to be the stable equilibrium position by properly locating the ball joint using Eqs. (51). Hence, a single-axis rotation, that is not affected by gravity, can be accomplished about any desired axis once the proper ball joint location has been determined.

The SCOLE design challenge maneuvers are time-optimal rotations beginning and ending in a state of rest. Provided the axis of rotation is the cable axis, the eigensolution of the structure before and after the maneuver will be the same. During the maneuver, the gyroscopic and stiffness matrices, and hence the eigenvalue problem, are functions of time. Solving the eigenvalue problem at each time step would be inefficient and of limited usefulness. However, a truncated set of the premaneuver eigenfunctions can be used as a set of admissible vectors to reduce the order of the equations of motion. The equations in reduced form can then be solved using a discrete-time technique.

A most desirable control technique for a maneuver excites the elastic modes as little as possible. The obvious method is to apply a force that is proportional to the rigid-body mode corresponding to the maneuver. Because the modes are orthogonal, the other modes are not excited. The control forces must be distributed throughout the structure to maintain it in its initial state of deformation. Of course, this would require distributed actuators and can only be approximated with discrete actuators, so that the elastic modes will be excited somewhat.

For simplicity, consider a rotation about the mass center in the direction of a principal axis. The equation governing such a maneuver can be expressed as

$$M_0(t) = a_0(t) I_0 \tag{52}$$

where $a_0(t)$ is the desired angular acceleration, $M_0(t)$ is the moment delivering this desired performance and I_0 is the mass moment of inertia. For reasons mentioned above, we wish to apply the moment by means of distributed actuators, so that $M_0(t)$ is the resultant moment produced by forces $F(p,t)$ distributed throughout the structure or

$$M_0(t) = \int_D r(p) \, F(p,t) \, dD(p) \tag{53}$$

Introducing the definition of I_0 and Eq. (53) into Eq. (52), the equation governing the maneuver can be expressed as

$$\int_D r(p)\ F(p,t)\ dD(p) = \int_D a_0(t)\ m(p)\ r^2(p)\ dD(p) \qquad (54)$$

where $r(p)$ is the distance from the mass center to point p, where $r(p)$ is normal to the axis of rotation, and $m(p)$ is the mass density of the structure at point p. Considering Eq. (54), and consistent with our desire for the force to be proportional to the rotational mode, the force density can be expressed as

$$F(p,t) = a_0(t)m(p)r(p) \qquad (55)$$

Because the force is proportional to the rotational mode, it is orthogonal to all of the other modes, so that it will excite only the desired rotational maneuver. Note that the force is also proportional to the mass, so that the mass acts as the control gain. This suggests that when this force is applied with discrete actuators, the actuators should be located at the point of maximum mass for maximum efficiency in rigid-body control.

5. Conclusions

The equations of motion for the structure both in orbit about the earth and in the laboratory are nonlinear, even when the elastic deformations are small. The nonlinear terms result from the large rigid-body maneuver. Through a perturbation approach, the nonlinear equations of motion can be transformed into a set of equations governing the rigid-body motions and a set of time-varying, linear equations governing small deviations from the prescribed rigid-body maneuver, as well as elastic motions. The first-order equations are non-self-adjoint. The mass matrix is time invariant so that it need only be inverted once in a discrete time simulation. The order of the equations can be reduced using the premaneuver eigenfunctions as admissible functions. For the laboratory experiment, a single-axis rotational maneuver, which is unaffected by gravity, is possible. The control force for the rigid-body rotation should be proportional to the corresponding rigid-body mode, with the mass acting as the control gain. Also, the actuators should be located at the points of maximum mass.

6. References

1. Meirovitch, L., _Computational Methods in Structural Dynamics_, Sijthoff-Noordhoff, The Netherlands, 1980.
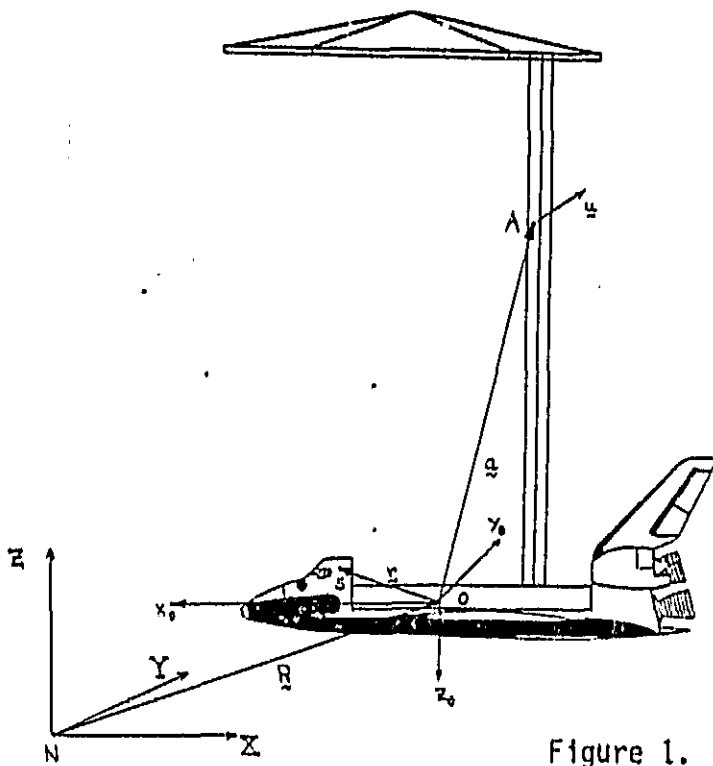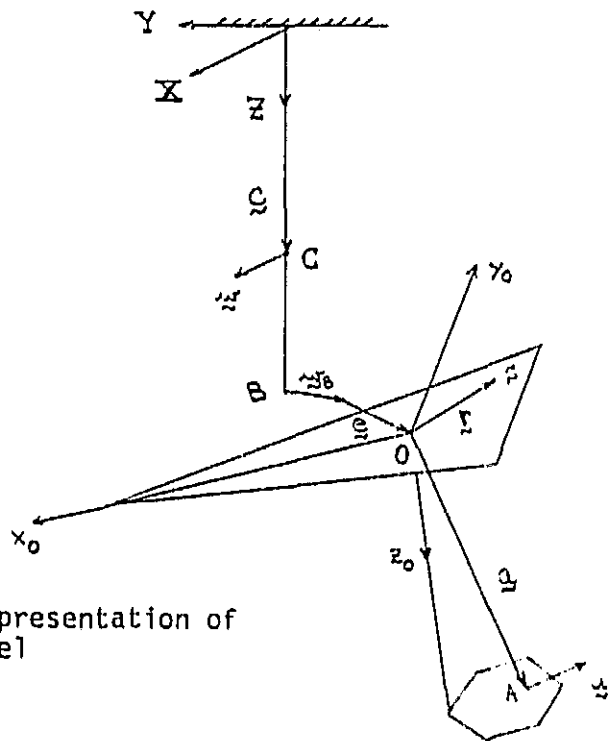2. Meirovitch, L., _Methods of Analytical Dynamics_, McGraw-Hill, New York, 1970.

Figure 1. SCOLE Configuration

Figure 2. Kinematical Representation of
Laboratory Model